Reply to Comment on "Conformational Changes and Aggregation of Alginic Acid as Determined By Fluorescence Correlation Spectroscopy"

ARTICLE *in* BIOMACROMOLECULES · FEBRUARY 2007

Impact Factor: 5.75 · DOI: 10.1021/bm060655d · Source: PubMed

Conformational Changes and Aggregation of Alginic Acid as Determined By Fluorescence Correlation Spectroscopy

Fabrice Avaltroni,[†] Marianne Seijo,[†] Serge Ulrich,[†] Serge Stoll,[†] and Kevin J. Wilkinson*[,‡]

Analytical and Biophysical Environmental Chemistry, University of Geneva, 30 Quai E. Ansermet, Geneva CH-1211, Switzerland, and Department of Chemistry, University of Montreal, P.O. Box 6128, succ. Centre-ville, Montreal, Quebec H3C 3J7, Canada

Received July 7, 2006; Revised Manuscript Received October 10, 2006

Insight into the conformations and aggregation of alginic acid was gained by measuring its diffusion coefficient at very dilute concentrations using fluorescence correlation spectroscopy. Both the pH and ionic strength (*I*) had an important influence on the diffusion coefficient of the polysaccharide. For pH, three effects were isolated: (i) below pH 4, the charge density decreased causing increased aggregation; (ii) between pH 4 and 8, a molecular expansion was observed with increasing pH, whereas (iii) above pH 8 some dissociation of the polymer was observed. Increasing *I* from 0.001 to 0.1 M resulted in a ca. 20% increase in the diffusion coefficient. By coupling these measurements to molar mass determinations obtained by size exclusion chromatography and monomer size estimations determined from ab initio calculations, it was possible to determine the radii of gyration via de Gennes renormalization theory. From diffusion coefficients and radii of gyration obtained as a function of ionic strength, persistence lengths (total, electrostatic, and intrinsic) were calculated from the Benoit−Doty relationship.

Introduction

Alginic acid is an unbranched polysaccharide consisting of (1→4)-linked residues of β-D-mannuronic acid (M) and its C5-epimer, α-L-guluronic acid (G). It can be found naturally at low concentrations in seawater, where it is secreted by several species of brown algae[1] and where it is believed to play a role in global carbon cycling. It is widely used in the food industry, due to its concentration-dependent ability to form gels.[2] For this reason, a majority of studies have focused on its gelling properties, at either molecular (e.g., "egg-box" model[3]) or macroscopic scales[4] with most of the studies being performed in semidilute or concentrated solutions.[5] However, few studies have been performed under the dilute conditions that are representative of its concentrations in natural waters. In these systems, the conformation of the individual polymer chains is expected to play a significant role in determining its physicochemical properties, including the circulation of suspended colloidal material.[6]

Polymer rigidity can be quantified by persistence lengths, L_p, which can be probed using techniques such as X-ray or neutron scattering, light scattering, rheology, microscopy, and more recently by ultrasonic wave spectroscopy.[7] With the exception of microscopy, the techniques are often limited to large molecules, high concentrations, or monodisperse systems. Microscopy techniques, while direct, must necessarily take into account the interaction of the biopolymer with a substrate.[8] An alternative technique, fluorescence correlation spectroscopy (FCS) is tailored to the study of dilute concentrations by measuring the diffusion times of near single molecules in solution.[9] Technical aspects, typical experimental setups, assumptions, and models have been reviewed recently.[10] In brief, by calibration of a laser-defined confocal volume through which molecules are allowed to diffuse, translational diffusion coefficients of fluorescent species can be measured. As diffusion coefficients are closely related to the size of the diffusing species, subtle changes in macromolecular sizes and conformations can be monitored as a function of the physicochemical properties of the solution. For example, in a previous study on Cd^{2+} and Pb^{2+} complexation by alginic acid,[11] the presence of the cations was found to have a significant impact on their conformations.

In this study, the aggregation, conformations, and rigidity of alginic acid were evaluated from the diffusion coefficients, radii of gyration, and persistence lengths as a function of pH and ionic strength. Persistence lengths were determined by combining measurements of diffusion coefficients obtained by FCS with molar mass measurements determined by size exclusion chromatography (SEC) and molecular simulations of monomer sizes. By probing persistence lengths as a function of ionic strength, it was possible to evaluate the intrinsic and electrostatic contributions to the persistence lengths of the biopolymer.

Theory

For linear polymers in good solvents, the diffusion coefficient, *D*, can be related to the radius of gyration, R_g, through de Gennes renormalization theory[12,13]

$$D \cong 0.0829 \frac{k_B T}{\eta R_g} \tag{1}$$

where k_B is Boltzmann's constant, *T* is the absolute temperature, and η is the solvent viscosity. For wormlike chains ranging from a random coil to a rigid rod, the Benoit−Doty equation[14] can be used to relate the radius of gyration to the persistence length, L_p

* Author to whom correspondence should be addressed. E-mail: kj.wilkinson@umontreal.ca.

[†] University of Geneva.

[‡] University of Montreal.

10.1021/bm060655d CCC: $37.00
Published on Web 12/10/2006

$$R_g^2 = \frac{1}{3}L_pL_c - L_p^2 + 2\frac{L_p^3}{L_c}\left(1 - \frac{L_p}{L_c}(1 - e^{-L_c/L_p})\right) \quad (2)$$

where L_c represents the total contour length of the polymer chain. In this paper, eq 2 was solved numerically for L_p by forcing the term on the right-hand side of the equation to converge with the R_g^2 value obtained from eq 1. The mean contour length is given by the product of the number-average monomer number $\langle N_{monomer}\rangle$ and the monomer length, $l_{monomer}$

$$\langle L_c\rangle = \langle N_{monomer}\rangle l_{monomer} \quad (3)$$

$\langle N_{monomer}\rangle$ can be determined by dividing the number-average molar mass of the biopolymer, M_n, by the mass of a monomer. The molar mass of both the M and the G (dehydrated) monomers of alginic acid is 176.9 g mol^{-1}.

The persistence length can be divided into two components reflecting the intrinsic persistence length, L_i, due to the local stiffness of the (uncharged) polymer backbone and the electrostatic persistence length, L_e, that is due to the intramolecular charge repulsion

$$L_p = L_i + L_e \quad (4)$$

Since the electrostatic persistence length depends on the charge screening of the biopolymer, it will vary with the physicochemical properties of the solution, in particular the ionic strength. The charge screening intensity can be evaluated from the Debye−Hückel parameter, κ[15]

$$\kappa = \sqrt{\frac{1000e^2N_A}{\epsilon\epsilon_0k_BT}\sum z_i^2C_i} \quad (5)$$

where e is the elementary charge ($e = 1.6 \times 10^{-19}$ C), N_A represents the Avogadro number ($N_A = 6.022 \times 10^{23}$ mol^{-1}), z is the charge of the electrolyte, C_i is the ionic concentration (mol L^{-1}), ϵ_0 is the vacuum permittivity ($\epsilon_0 = 8.85 \times 10^{-12}$ C V^{-1} m^{-1}), and ϵ is the water relative permittivity. The electrostatic persistence length can be plotted against the Debye length, κ^{-1}, raised to an exponent (α) that depends upon the chemical structure and charge screening effects on the polymer.[16] For flexible polymers, the exponent is generally ≥ 1[16,17] and approaches 2.0 for rigid polymers.[18]

Materials and Methods

Products. Alginic acid (*Macrocystis pyrifera*, medium viscosity, A2033) was purchased from Sigma (St. Louis, MO); sodium nitrate (≥99.0%) was bought from Fluka; rhodamine 123 (R123, >99%), rhodamine 6G (R6G, 99%), and sodium cyanoborohydride were purchased from Acros Organics (Geel, Belgium). Water was always Milli-Q quality (R > 18 MΩ cm, organic carbon < 2 μg C L^{-1}). High-purity sodium chloride, sodium hydroxyde, and nitric acid (various suppliers) were used for pH and ionic strength adjustments.

Alginic acid (AA) samples were prepared at 0.05 or 0.1 g L^{-1} using $NaNO_3$ to set the ionic strength between 10^{-3} and 10^{-1} M. The pH was adjusted with 0.1 M NaOH or HNO_3. Samples were partially sterilized, and large aggregates were removed by 0.22 μm filtration. In the FCS experiments, 15 μL of purified, derivatized alginic acid (see below, final concentration 2.2×10^{-6} g L^{-1}) was added to 10 mL of unlabeled AA (final concentration 0.05−0.1 g L^{-1}) then left to equilibrate overnight prior to measurements.

Derivation of the Alginic Acid. Alginic acid was derivatized using a two-step reductive amination (Figure 1).[18] In brief, 1 equiv of alginic acid (0.0529 g for a molar mass of 100 000 g mol^{-1}) was dissolved in 10 mL water. After dissolution, 0.1 M HCl was added to bring the sample to pH 5. Rhodamine 123 (33 equiv, 6.6×10^{-3} g) was dissolved in 1 mL of ethanol. The solution of R123 was added to the alginic acid then held at 70 °C for 30 min to react the primary amine of the R123 with the carbonyl moiety of the hemi-acetal form of the alginic acid end group. Sodium cyanoborohydride, $NaCNBH_3$ (45 equiv, 1.5×10^{-3} g), was dissolved in 1 mL of dimethyl formamide (DMF) and added to the reaction mixture where it was left for 60 min at 70 °C to reduce the imine intermediate to a secondary amine. For the purification step, 1 mL of the reaction mixture was precipitated in 5 mL of ethanol and 200 μL of 0.1 M $NaNO_3$. The precipitate was carefully transferred to another vial where the dissolution and precipitation procedures were repeated (2×). The labeled alginate was diluted in 3 mL of water (e.g., 3× dilution) to give a final concentration of 1.47×10^{-3} g L^{-1}. The labeling procedure was previously demonstrated to be nonperturbing with respect to the macromolecular conformations of a number of polysaccharides.[18]

Fluorescence Correlation Spectroscopy. Fluorescence was measured using an avalanche photodiode detector on a Confocor Axiovert 135TV FCS (Carl Zeiss). An optimized setting of 12 × 90 s acquisitions was used, implying a total irradiation time of 18 min for each sample. Excitation of the fluorophore was accomplished using an Ar^+ laser at 514 nm, corresponding closely to the maximum excitation wavelength for the rhodamine derivative. All experiments were performed at 22.5 °C.

Fluorescence intensity variations inside the confocal volume can be attributed to the Brownian motion of a fluorophore through a laser-defined confocal volume. Diffusion times, τ, are determined by calibrating the dimensions of the confocal volume (~1 μm^3) using R6G, which has a known diffusion coefficient of 2.8×10^{-6} cm^2 s^{-1} in water,[19] and analyzing data using an autocorrelation function, $G(t)$. For a single-component system, in the absence of phosphorescence, $G(t)$ can be related to τ

$$G(t) = a + \frac{1}{n}\left(1 + \frac{t}{\tau}\right)^{-1}\left(1 + \frac{t}{p^2\tau}\right)^{-0.5} \quad (6)$$

where a is the limiting value of $G(t)$ for $t \rightarrow \infty$ (usually $a = 1$), n is the average number of fluorescent particles diffusing in the confocal volume, τ is the diffusion time of the species inside the confocal volume, and p is the structure parameter (ratio of the transversal, ω_{xy}, to longitudinal, ω_z, radius of the confocal volume) obtained from the calibration. If two types of fluorescent molecules are present in the sample (e.g., labeled macromolecule and free fluorophore), then eq 7 can be expanded to include both species[10]

$$G(t) = a + \frac{1}{n}\left\{(1-y)\left(1 + \frac{t}{\tau_1}\right)^{-1}\left(1 + \frac{t}{p^2\tau_1}\right)^{-1/2} + y\left(1 + \frac{t}{\tau_2}\right)^{-1}\left(1 + \frac{t}{p^2\tau_2}\right)^{-1/2}\right\} \quad (7)$$

where y is the fraction of signal due to the second species and τ_1 and τ_2 are the diffusion times of the first and second species, respectively. In this study, due to the unavoidable presence of unreacted R123 in the solution of labeled alginic acid, the two-component model (eq 7) was generally used. Thus, a typical experimental series consisted of: (i) 12 measurements of R6G in water to calibrate the confocal volume, (ii) 12 measurements of rhodamine 123 in water to determine its diffusion time (eq 6) for subsequent use as τ_2 in eq 7, and (iii) 12 measurements of each of the samples. Number-average diffusion coefficients were determined from the measured diffusion times across the calibrated confocal volume.

Molar Mass Determinations. Molar mass distributions were determined by size exclusion chromatography on 100 μL of a 1 g L^{-1} solution of alginic acid. The chromatographic system consisted of three Shodex 8 mm × 300 mm OH-Pak columns (SB-802.5, SB-803, SB-804) placed in series after a SB-G 6 mm × 50 mm guard column. A

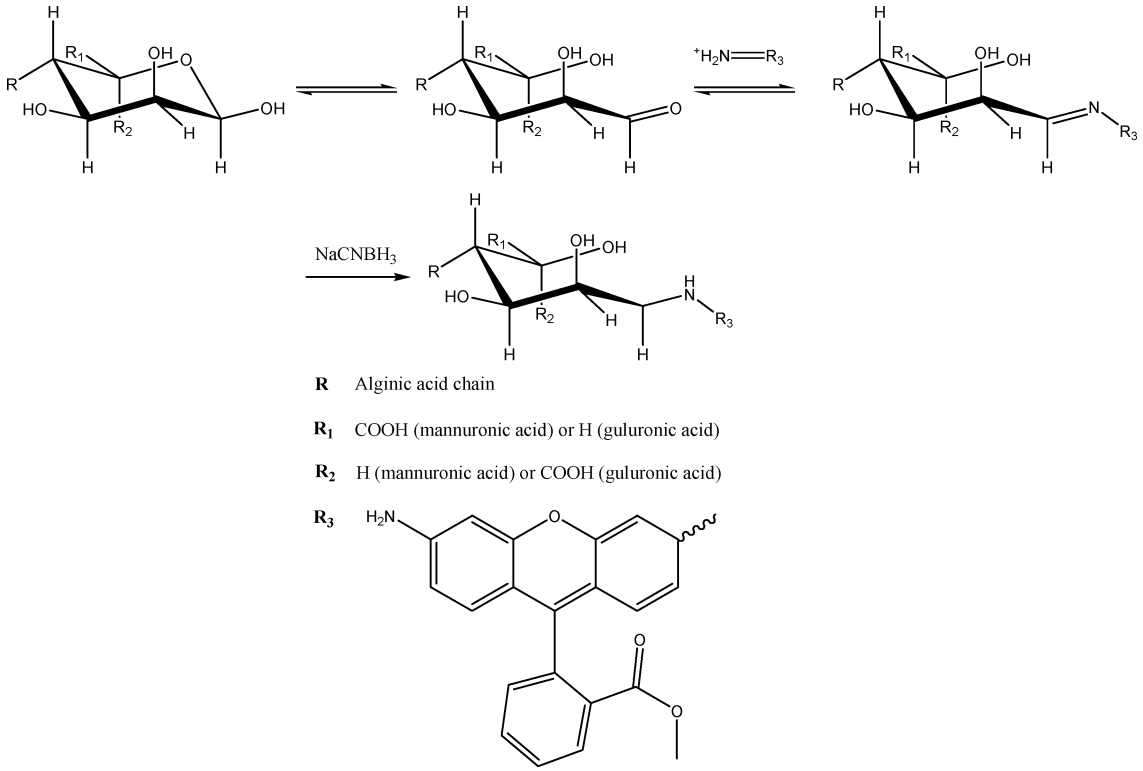

Figure 1. Derivatization of the terminal sugar of the alginic acid using rhodamine 123.

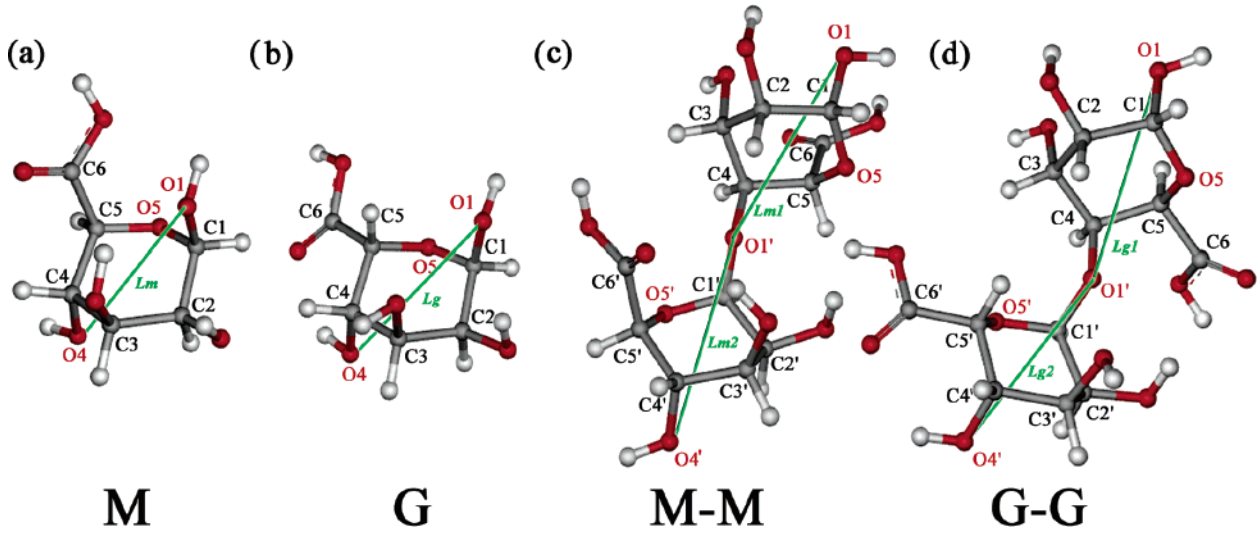

Figure 2. Atomic and monomer lengths and numbering of (a) β-D-mannuronic acid (M), (b) β-D-guluronic acid (G), (c) β-D-(1→4)-mannuronan disaccharide (M−M), and (d) β-D-(1→4)-guluronan disacchride (G−G).

0.1 M NaCl solution at a flow rate of 0.6 mL min^{-1} was used as the eluent. Detection was performed using a Merck RI-71 differential refractometer (Merck, Germany). Calibration of the device was performed with monodisperse pullulan standards between 5900 and 788 000 g mol^{-1}. All measurements were made at room temperature (T = 22.5 °C).

^{1}H NMR Determination of the M/G Ratio. The frequency of occurrence of the G monomer, F_G, was determined from ^{1}H NMR peak intensities[20,21] following sample depolymerization.[22,23] With 0.1 M HCl to adjust the pH, samples (0.333 g L^{-1}) were brought to 95 °C and left 1 h at pH 5.6 and 45 min at pH 3.8. Finally, the solution was neutralized (pH 7) with 0.1 M NaOH, lyophilized, and redissolved (2×) in D_2O. The ^{1}H NMR experiment was performed on a Bruker 500 MHz NMR using an acquisition time of 3.17 s, a sample window of 10 330 Hz, a line broadening of 0.3 Hz, and a temperature of 90 °C.

Computational Procedures. Monomer lengths (Figure 2) were determined for the β-D-mannuronic acid (M) and β-D-guluronic acid (G) monomers and for the β-D-(1→4)-mannuronan (M−M) and β-D-(1→4)-guluronan (G−G) disaccharides. Calculations were performed using the Gaussian 98 series of programs using ab initio and density functional theory (DFT) calculations.[24] Quantum calculations were carried out by geometrical optimization and vibrational analysis on a restricted Hartree Fock (RHF) with a 6-31G* basis set. Geometrical reoptimization was performed with the hybrid functional B3LYP[25] on a 6-31G* basis set to take into account the dynamic correlation of the electrons on the geometry. Comparisons of the total energy were performed to obtain the best geometry of the monomers. Energies were also calculated with B3LYP/6-311++G to reduce the basis set superposition error (BSSE) in the hydrogen-bonding energy calculation,[26] a manipulation that appears to deliver the best potential energy surfaces for carbohydrates.

Saccharides and disaccharides were studied to include connectivity

Table 1. Monosaccharide and Disaccharide Bond Lengths in Their Minimal Configurations Calculated at Different Ab Initio Quantum Chemical Calculation Levels and the Corresponding Energies[a]

species	RHF/6-31G*	B3LYP/6-31G*	B3LYP/6-311++G**
		Monosaccharide M	
Lm (Å)	4.430	4.523	4.523
energy (hartree)	−757.050	−761.184	−761.261
		Monosaccharide G	
Lg (Å)	4.509	4.560	4.560
energy (hartree)	−757.053	−761.186	−761.457
		Disaccharide M−M	
*Lm*1/*Lm*2 (Å)	4.495 / 4.486	4.480 / 4.542	4.480/4.542
energy (hartree)	−1438.085	−1445.959	−1446.448
		Disaccharide G−G	
*Lg*1/*Lg*2 (Å)	4.527 / 4.514	4.582 / 4.557	4.582 / 4.558
energy (hartree)	−1438.087	−1445.951	−1446.086

[a] Quantum calculations were carried out with a restricted Hartree Fock (RHF) with a 6-31G* basis set. Geometrical reoptimization was performed with the hybrid functional B3LYP[43] on a 6-31G* basis set. Energies were calculated with B3LYP/6-311++G. *Lm*, *Lg*, *Lm*1, *Lm*2, *Lg*1, and *Lg*2 correspond to the monomer unit dimensions (cf. Figure 2) (1 hartree = $4.3597482 \times 10^{-18}$ J).

effects between the monomers. In disaccharides, the relative orientation of the two residues was determined by the dihedral angles Φ and ψ as defined by HC1−C1−O1−C3′ and C1−O1−C3′−HC3′ (Figure 2). Angular conformations for the disaccharides were optimized in the molecular mechanics calculations using the grid search method of Braccini et al.[27]

Results and Discussion

Some of the physicochemical properties of alginic acid were measured to characterize the sample. The water content determined by oven drying at 100 °C until constant weight was 19.8% (w/w), in line with previous values of 10−25%.[42] The carboxylic acid content was measured by titration (4.40×10^{-3} mol g^{-1} [11]) and was similar to literature values ($4.50 \times 10^{-3} \pm 0.03 \times 10^{-3}$ mol g^{-1};[28] 4.39×10^{-3} mol g^{-1} [29]). A single pK_a value of 3.44 could be distinguished, in line with values that would be determined for the M (3.2−3.28) or G (3.6−3.65) homopolymers.[2,3,30] An M/G ratio of 1.61 was determined by NMR, close to the expected M/G ratio (1.43−1.56[2]) obtained for samples of alginic acid isolated from *M. pyrifera*.

Computational Results. Monomer lengths for both the G and the M monomers and the G−G and M−M disaccharide lengths are presented in Table 1. The calculated O−O distances were similar for the monosaccharides and disaccharides, and thus an average monomer length of 4.537 Å was determined by weighting the calculation with respect to the measured M/G ratio. This value is slightly lower than the bond length of 4.83 Å that was determined by X-ray fiber diffraction[31] for an alginic acid from the same source. In that case, the estimate referred to a hydrated and crystallized structure whereas the ab initio results here refer to an in vacuo value. It is thus reasonable to conclude that, in solution, the monomer lengths are in the 4.6−4.8 Å range.

Molar Mass Distribution. Average molar masses were calculated from distributions obtained from size exclusion chromatography. Alginic acid showed a bimodal molar mass distribution in relative proportions of 10% and 90% (w/w) (Figure 3) with the first peak roughly centered on the mass of the monomer. Elsewhere, this peak has been described as an impurity containing polyols, monomers, and ionic species.[33] The second, larger peak had a broad molar mass distribution from 2×10^3−10^7 g mol^{-1}. In the following, average molar masses will be determined by considering only the second peak.

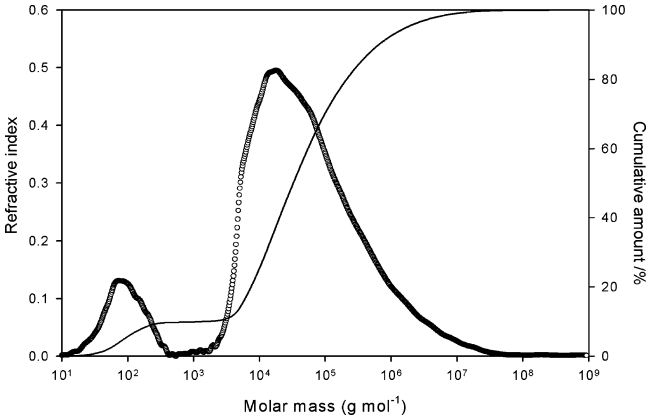

Figure 3. Size exclusion chromatography of the alginic acid used in this study: (a) refractive index (RI) signal (○); (b) cumulative RI signal (solid line). The first peak accounts for 10% of the total mass distribution.

The number-average molar mass, M_n, was determined as 19.2 kg mol^{-1}, lower than the majority of molar mass distributions found in the literature (Table 2). However, the weight average molar mass, M_w, of 989 kg mol^{-1} was generally larger than the literature values. The broad molar mass distribution reflected an important polydispersity (polydispersity factor, $p = 51.46$) for the raw alginic acid, in agreement with what has been observed in other studies.[34] The observed differences may be due to the fact that the alginic acid employed here was not extensively purified. Other factors, such as the algal strain and isolation process,[2] may also have an effect on the molar masses. On the basis of the number-average molar mass, the contour length was estimated to be 50 nm (eq 3).

Influence of the Ionic Strength on the Conformation of Alginic Acid. In the interpretation of FCS results, the two-component model is only valid if diffusion coefficients of the two components are sufficiently separated (i.e., diffusion times differ by a factor greater than 1.6 for similar quantum yields[38]). This was indeed the case in this study since the diffusion time of the alginic acid was 7.4 ± 0.5 times greater than that of the free fluorophore.

A 20% increase in the average diffusion coefficient of the alginic acid, corresponding to a 20% decrease in the gyration radius (eq 1), was observed as the ionic strength increased from 10^{-3} to 10^{-1} M (Figure 4). A similar trend was observed for both alginic acid concentrations that were examined (0.05 and

Table 2. Average Molar Masses, Polydispersities (p), and M/G ratios (Expressed as Frequency of G Monomer, F_G, and Frequency of G−G Dimer, F_{G-G}) Published for Various Alginic Acids in the Literature

M_n (g/mol)	M_w (g/mol)	M_v (g/mol)	p	F_G/F_{G-G}	reference
0.1922×10^5	9.89×10^5		51.4	0.38/0.24	this work
	2.13×10^5		2.0	0.42/0.20	31
$0.63 \times 10^5 - 2.12 \times 10^5$				>0.6	35
$0.84 \times 10^5 - 1.2 \times 10^5$	$2.07 \times 10^5 - 2.1 \times 10^5$		1.7−2.6		2
7.1×10^3			1.6		34
		$(0.167 \pm 0.09) \times 10^5$		0.45	28
$0.569 \times 10^5 - 2.006 \times 10^5$	$1.150 \times 10^5 - 3.217 \times 10^5$		1.53−3.25		36
	8×10^5				37

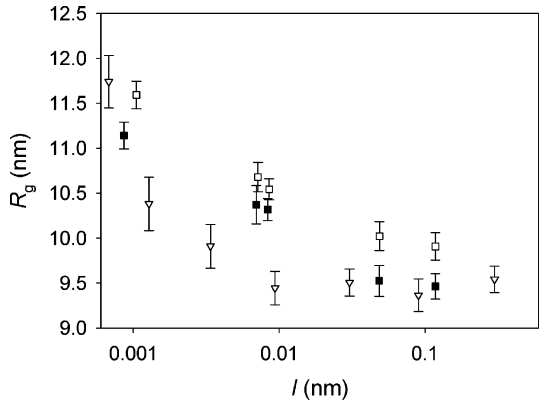

Figure 4. Effect of the ionic strength on the radius of gyration, R_g, of alginic acid. Values were calculated from measurements of the diffusion coefficients made at pH 6.0 using eq 1. Ionic strength was adjusted with NaCl for samples containing (■) 0.05 g L^{-1} alginic acid and (□) 0.1 g L^{-1} alginic acid and with $MgCl_2$ (▽) for a sample containing 0.1 g L^{-1} alginic acid.

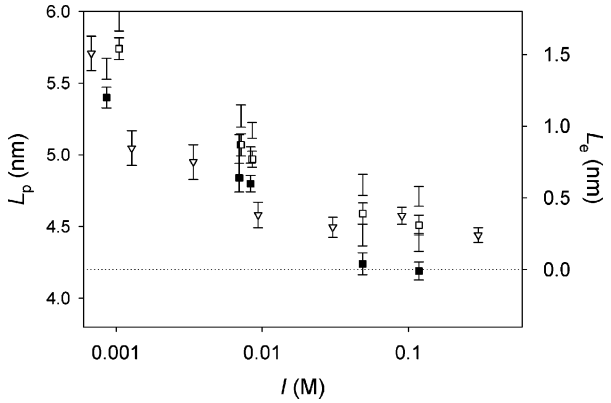

Figure 5. (a) Total persistence lengths calculated from the Benoit−Doty equation (left-hand scale) and electrostatic persistence lengths determined from eq 4 (right-hand scale). The dotted line corresponds to the intrinsic persistence length under the assumption that the polymer is completely screened above 0.1 M. Ionic strength was adjusted with NaCl for samples containing (■) 0.05 g L^{-1} alginic acid and (□) 0.1 g L^{-1} alginic acid and with $MgCl_2$ (▽) for a sample containing 0.1 g L^{-1} alginic acid.

0.1 g L^{-1}). The value of the radius of gyration reached a minimum (ca. 9.3 nm) at high ionic strengths (ca. >0.1 M).

Upon the basis of the calculated contour length of 49.6 nm, persistence lengths determined from eq 2 ranged from 4 to 6 nm (Figure 5). At a relatively low ionic strength of 1 mM, the persistence length was between 5.4 and 5.8 nm, while at high ionic strengths the value decreased to as low as 4.0 nm (not all data or replicates are shown). The slightly larger sizes (Figure 4) and persistence lengths (Figure 5) that were observed for the higher concentration (0.1 g mol^{-1}) of AA, if significant, can be attributed to a very small amount of aggregation in the more concentrated solution. Literature values of persistence lengths vary greatly as a function of solvent conditions, the M/G ratio of the alginic acid, molar masses, the polymer characterization technique, and the mathematical assumptions employed for determining the persistence lengths. For example, values of 12.6[39] and 15.2 nm[31] have been determined by rheology while persistence lengths of 9 ± 1 nm[40] and 16 ± 7 nm[41] were measured by electron microscopy for alginic acids of unspecified M/G ratios. The values observed here are of a similar order of magnitude as those found by tapping mode atomic force microscopy (AFM) where values of 5−17 nm[42] were found for an alginic acid of 450 kg mol^{-1}. It should be noted that the microscopy techniques may potentially lead to an overestimation of the persistence lengths since the sample is strictly considered as an adsorbed two-dimensional object, while its real state is intermediate between two- and three-dimensional.[40] Finally, a persistence length of 5.2 nm was determined when SEC was combined with triple detection (viscometry, refractive index, and light scattering).[34] Upon the basis of the persistence lengths that varied between 4 and 6 nm and the estimated contour length of 49.6 nm, it can be concluded that the alginic acid had a semiflexible structure under all of the conditions that were examined here.

Contributions to the polymer rigidity were due to both intrinsic chemical and electrostatic components. At the highest (NaCl) ionic strength examined, i.e., 118 mM, the Debye length, κ^{-1}, was <0.1 nm, and charges could be considered to be effectively screened. FCS measurements are practically limited to electrolyte concentrations below ca. 300 mM, since above this concentration the confocal volume can change significantly due to variations in the refractive index of the solution. Nonetheless, above 100 mM, the total persistence length could be equated to the intrinsic persistence length, L_i, under the assumption that the electrostatic persistence length, L_e, was zero. Indeed, at the highest ionic strengths examined, results obtained using $MgCl_2$ to adjust the ionic strength (i.e., higher ionic strengths for similar electrolyte concentrations) confirmed the observation of a constant L_p, similar to results obtained using NaCl (Figure 5). Upon the basis of these assumptions, an intrinsic persistence length of ca. 4.2 nm could be estimated, corresponding to ca. 9−10 monomers. At the lowest ionic strength examined here (0.86 mM), the electrostatic persistence length was estimated to be 1.5 ± 0.1 nm, accounting for 22% of the total persistence length.

Under the assumption of a wormlike chain ($L_k = 2L_p$), the results are in good agreement with Kuhn length (L_k) determinations of 10 ± 6 nm obtained by dynamic light scattering[43] for an alginic acid sample having a similar M/G ratio and molar mass ($M_w = 1.9 \times 10^5$ g mol^{-1}) and tested under similar conditions (pH = 6.3, I = 95 mM). Furthermore, the results

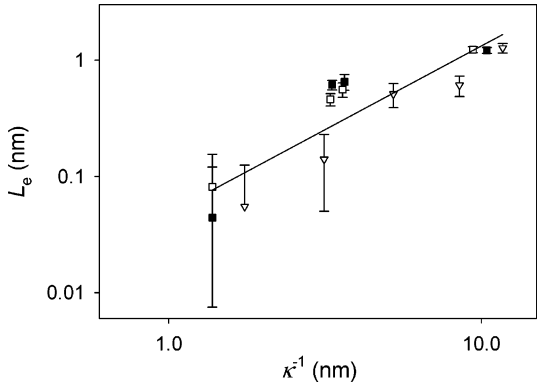

Figure 6. Logarithm of the electrostatic persistence lengths as a function of the logarithm of the Debye−Hückel screening length obtained from diffusion coefficient measurements at pH 6.0. Ionic strength was adjusted with NaCl for samples containing (■) 0.05 g L^{-1} alginic acid and (□) 0.1 g L^{-1} alginic acid and with $MgCl_2$ (▽) for a sample containing 0.1 g L^{-1} alginic acid. The slope of the log−log plot was 1.44 ± 0.15 ($R^2 = 0.81$).

correspond well to those of Zhang et al.[39] who observed that L_e decreased from 3.24 nm at 10 mM to 0.065 nm at 500 mM ionic strength. The slight differences with respect to our results could be explained by the use of different salts[44] and alginic acids having different M/G ratios. Indeed, the frequency of M−G dimers in the alginic acid has been shown to cause kinks in the structure,[45] which are likely to affect both R_g and L_p. The plot of the (log) electrostatic persistence length versus the (log) Debye length, κ^{-1}, gave a slope of 1.44 ± 0.15, which was consistent with the L_p determinations indicating a semiflexible structure (Figure 6).

Influence of the pH on the Conformation of Alginic Acid and the Formation of Aggregates. Three major trends were observed for the variation of R_g and L_p as a function of pH (Figure 7). In the pH range from 8 to 4 (Figure 7, zone ii), a slight decrease in R_g and L_p was observed as the pH approached the pK_a of the molecule, i.e., pH of 3.2−3.65.[1,2,30] Protonation of the alginic acid is expected to decrease the intramolecular electrostatic repulsion, resulting in a small reduction in molecular rigidity and size that is reflected by the decrease in L_p and R_g. As the molecule is protonated further below pH 4, the increase in size is interpreted as a limited aggregation (40% increase in average size) due to the reduction in intermolecular repulsion (greatly overwhelming any size decrease due to the reduction in intramolecular repulsion) (Figure 7, zone i). In this zone, the observed increase in the gyration radius cannot be directly translated as an increase in the molecular persistence lengths since we are no longer considering isolated chains. Above pH 8.0, a 20−30% decrease in size was observed that was attributed to the depolymerization of alginic acid by a β-alkoxy-elimination mechanism and formation of small more flexible fragments (Figure 7, zone iii).[46]

Conclusion

FCS measurements were coupled to molar mass (SEC) and monomer size (ab initio determinations) to evaluate the rigidity and conformation of an alginic acid as a function of both pH and ionic strength. Estimates of gyration radii as well as the intrinsic and electrostatic persistence lengths showed that alginic acid behaved as a semiflexible polymer, in agreement with previous assessments. For alginic acid, the electrostatic persistence length represented up to 22% of the total persistence length at ionic strengths of 1 mM, decreasing to a negligible contribution above 100 mM. A screening of the molecular charges by the salt resulted in a reduction in both the gyration radius and the persistence length, indicative of a more compact structure. Protonation of the carboxylic functional groups had a similar effect on the persistence length of the alginic acid to pH 4.0. Below pH 4.0, the reduction in molecular charge resulted in a significant aggregation. At these pH values, the increased size due to aggregation overwhelmed the decreased size due to increased molecular flexibility. Under alkaline conditions, the hydrodynamic radius of the alginic acid decreased, likely due to a depolymerization of the polysaccharide chains.

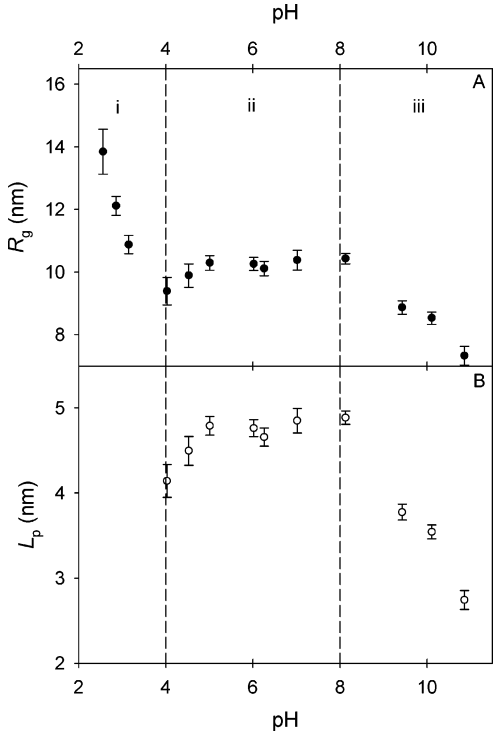

Figure 7. (a) Influence of pH on the calculated radii of gyration and (b) persistence lengths of alginic acid for 0.1 g L^{-1} alginic acid at an ionic strength of 50 mM. Three different regimes describing the behavior of the AA molecules are thought to occur: (i) aggregation of highly protonated alginic acid molecules; (ii) reduction in molecular rigidity due to a decreased intramolecular electrostatic repulsion; (iii) depolymerisation. See text for further details.

Acknowledgment. V. Normand, P.-Y. Morgantini, and T. A. Davis are thanked for helpful discussion. M. Chevalier and P.-E. Bouquerand are acknowledged for their assistance with the chromatographic characterization of the molar masses. This work was funded by the Swiss National Funds and the National Science and Engineering Research Council of Canada.

References and Notes

(1) Draget, K. I. In *Handbook of Hydrocolloids*; Phillips, G. O., Williams, P. A., Eds.; Woodhead Publishing: Cambridge, U. K., 2000; pp 379−395.
(2) Moe, S. T.; Draget, K. I.; Skjaek-Braek, G.; Smidsrod, O. *Food Sci. Technol. (New York)* **1995**, *67*, 245−286.
(3) Braccini, I.; Perez, S. *Biomacromolecules* **2001**, *2*, 1089−1096.
(4) Day, D. F. In *Biopolymers from Renewable Resources*; Kaplan, D. L., Ed.; Springer: Berlin, 1998; pp 119−143.
(5) Smidsrod, O.; Haug, A. *Biopolymers* **1971**, *10*, 1213−1227.
(6) Wilkinson, K. J.; Reinhardt, A. In *Flocculation in Natural and Engineered Environmental Systems*; Droppo, I. G., Leppard, G. G., Liss, S. N., Milligan, T., Eds.; CRC Press: Boca Raton, FL, 2005; pp 143−170.
(7) Aeberhardt, K.; de Saint-Laumer, J. Y.; Bouquerand, P. E.; Normand, V. *Int. J. Biol. Macromol.* **2005**, *36*, 275−282.

(8) Balnois, E.; Wilkinson, K. J. *Colloids Surf., A* **2002**, *207*, 229−242.
(9) Thompson, N. L. In *Topics in Fluorescence Spectroscopy*; Plenum Press: New York, 1991; Vol. 1, pp 337−378.
(10) Krichevsky, O.; Bonnet, G. *Rep. Prog. Phys.* **2002**, *65*, 251−297.
(11) Lamelas, C.; Avaltroni, F.; Benedetti, M.; Wilkinson, K. J.; Slaveykova, V. I. *Biomacromolecules.* **2005**, *6*, 2756−2764.
(12) Teraoka, I. *Polymer Solutions: An Introduction to Physical Properties*; John Wiley and Sons: New York, 2002.
(13) Oono, Y.; Kohmoto, M. *J. Chem. Phys.* **1983**, *78*, 520.
(14) Benoit, H.; Doty, P. *J. Phys. Chem.* **1953**, *57*, 958−963.
(15) Hiemenz, P. C.; Rajagopalan, R. *Principles of Colloid and Surface Chemistry*, 3rd ed.; Marcel Dekker: New York, 1997.
(16) Micka, U.; Kremer, K. *J. Phys.: Condens. Matter* **1996**, *8*, 9463−9470.
(17) Ullner, M.; Jönsson, B.; Peterson, C.; Sommelires, O.; Söderberg, B. *J. Chem. Phys.* **1997**, *107*, 1279.
(18) Meunier, F.; Wilkinson, K. J. *Biomacromolecules* **2002**, *3*, 857−864.
(19) Magde, D.; Elson, E. L.; Webb, W. W. *Biopolymers* **1974**, *13*, 29−61.
(20) Grasdalen, H.; Larsen, B.; Smidsrod, O. *Carbohydr. Res.* **1979**, *68*, 23−31.
(21) Grasdalen, H. *Carbohydr. Res.* **1983**, *118*, 255−260.
(22) Davis, T. A.; Mucci, A.; Volesky, B.; Llanes, F.; Diaz-Pulido, G.; McCook, L. *Appl. Biochem. Biotechnol., Part A* **2003**, *110*, 75−90.
(23) Davis, T. A.; Ramirez, M.; Mucci, A.; Larsen, B. *J. Appl. Phycol.* **2004**, *16*, 275−284.
(24) Parr, R. G.; Yang, W. In *Density Functional Theory of Atoms and Molecules*; Oxford University Press: New York, 1989.
(25) Becke, A. D. *Phys. Rev. A: At., Mol., Opt. Phys.* **1988**, *38*, 3098−3100.
(26) Lii, J. H.; Ma, B.; Allinger, N. L. *J. Comput. Chem.* **1999**, *20*, 1593−1603.
(27) Braccini, I.; Grasso, R. P.; Perez, S. *Carbohydr. Res.* **1999**, *317*, 119−130.
(28) DeRamos, C. M.; Irwin, A. E.; Nauss, J. L.; Stout, B. E. *Inorg. Chim. Acta* **1997**, *256*, 69−75.
(29) Fukushima, M.; Tatsumi, K.; Wada, S. *Anal. Sci.* **2001**, *17*, 663−666.
(30) Stefansson, M. *Anal. Chem.* **1999**, *71*, 2373−2378.
(31) Donati, I.; Coslovi, A.; Gamini, A.; Skjaek-Braek, G.; Vetere, A.; Campa, C.; Paoletti, S. *Biomacromolecules* **2004**, *5*, 186−196.
(32) Becke, A. D. *Phys. Rev. A: At., Mol., Opt. Phys.* **1988**, *38*, 3098−3100.
(33) Campa, C.; Oust, A.; Skjak-Braek, G.; Paulsen, B. S.; Paoletti, S.; Christensen, B. E.; Ballance, S. *J. Chromatogr., A* **2004**, *1026*, 271−281.
(34) Lee, K. Y.; Bouhadir, K. H.; Mooney, D. J. *Biomacromolecules* **2002**, *3*, 1129−1134.
(35) Neiss, T. G.; Cheng, H. N. In *NMR Spectroscopy of Polymers in Solution and in the Solid State*; Cheng, H. N., English, A. D., Eds.; ACS Symposium Series 834, American Chemical Society: Washington, DC, 2003; pp 382−395.
(36) Turquois, T.; Gloria, H. *J. Agric. Food Chem.* **2000**, *48*, 5455−5458.
(37) Smidsrod, O.; Haug, A. *Acta Chem. Scand.* **1968**, *22*, 797−810.
(38) Meseth, U.; Wohland, T.; Rigler, R.; Vogel, H. *Biophys. J.* **1999**, *76*, 1619−1631.
(39) Zhang, L.; Cai, J.; Zhou, J.; Tang, Y. *Sep. Sci. Technol.* **2004**, *39*, 1203−1219.
(40) Stokke, B. T.; Brant, D. A. *Biopolymers* **1990**, *30*, 1161−1181.
(41) Stokke, B. T.; Elgasaeter, A.; Skjaek-Braek, G.; Smidsrod, O. *Carbohydr. Res.* **1987**, *160*, 13−28.
(42) Maurstad, G.; Danielsen, S.; Stokke, B. T. *J. Phys. Chem. B* **2003**, *107*, 8172−8180.
(43) Strand, K. A.; Boe, A.; Dalberg, P. S.; Sikkeland, T.; Smidsrod, O. *Macromolecules* **1982**, *15*, 570−579.
(44) Volk, N.; Vollmer, D.; Schmidt, M.; Oppermann, W.; Huber, K. In *Polyelectrolytes with Defined Molecular Architecture II*; Schmidt, M., Ed.; Advances in Polymer Science 166; Springer: Berlin, 2002; pp 30−65.
(45) Decho, A. W. *Carbohydr. Res.* **1999**, *315*, 330−333.
(46) Smidsrod, O.; Haug, A.; Larsen, B. *Acta Chem. Scand.* **1966**, *20*, 1026−1034.

BM060655D